

Impact of Multiple Responses to a Single Sonication when Determining Nanobubble Contrast Agent Characteristics

M.R. Smith^{1,2} and C. Pellow²

¹Electrical and Software Engineering, Schulich School of Engineering, University of Calgary, Calgary, Canada

²Radiology, Cumming School of Medicine, University of Calgary, Calgary, Canada

Abstract— Multiple scatter responses were observed in a phantom channel containing nanobubble contrast agent following a single sonication, with agent replacement between trials changing the responses' relative positioning and intensities. Experimentally, the combined spectrum of several responses can show split peaks instead of a single peak at the sonication's carrier frequency. This is the result of the real and imaginary components of the complex-valued frequency spectra of individual scatter responses combining in a constructive or destructive manner. In some trials, changes towards a stable state were observed in agent longevity with a time constant of 2.5 milliseconds during multiple sonications. This paper applies two measures to determine whether this longevity variability is real or an algorithmic artefact due to minor position shifts of several scatter responses modifying the way their real and imaginary spectral components interfere. The first power measure determines the spectrum from all phantom data undistorted by reflections from the channel boundaries. The second measure determines the short-term Fourier transform of the hydrophone signal with an analysis window the length of the sonication moved across the full agent response, potentially capturing changes in individual scatter responses. Combining the results from the two metrics suggests that the changes in agent longevity metrics following multiple sonications are being impacted by the shape changes in the multi-peak spectra during a given trial.

Keywords— Agent longevity, Nanobubble contrast agent, Sonication responses, Spectral analysis artefacts.

I. INTRODUCTION

Preferential detection of the non-linear bubble response of a contrast agent and the cancellation of the background tissue signal forms the basis behind the ultrasound contrast imaging [1]. There is research interest in whether a change in the exciting sonication envelope's shape or length can better optimize the tissue-agent contrast when applying one of the phase inversion (PI) [2, 3], amplitude modulation (AM) [4, 5] or combined phase inversion – amplitude modulation (PIAM) [1, 6, 7] imaging schemes.

The time signals in **Fig. 1** show three representative responses from each of the multiple trials at 500 kPa, one component of a nanobubble agent phantom study at pressures between 100 - 1000 kPa regenerated from data supplied courtesy of the authors of [8]. Imagine that each of the three

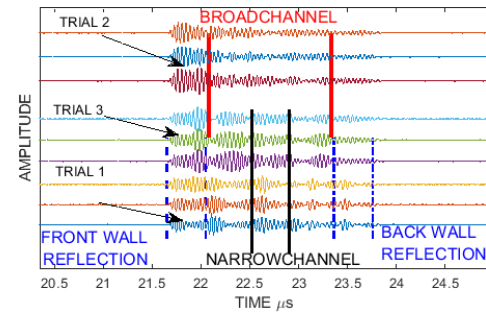


Fig. 1. The strength and positions of the components of three example responses to a single sonication differ between trials at 500 kPa. Scatter response lengths in the nanobubble contrast agent are both longer and shorter than the excitation pulse length, 400 ns, shown schematically bounded by the *black lines* labelled *NARROWCHANNEL* [8]. The *BROADCHANNEL* (bounded by *red lines*) indicates all data not distorted by the phantom's wall reflections. The arrows indicate where a scatter response early in the channel is overlapping the strong front wall reflections and changing its appearance through destructive interference.

trials in **Fig. 1** had been involved a different imaging scheme. Together the trials would then form an initial comparison study evaluating the relative differences in the spectral power present in the scatter responses as a measure of agent-tissue contrast. Following the experimental protocols described in [1, 8], the agent in the flow-through phantom was replaced between trials. This avoids introducing systematic errors associated with changes in the agent's longevity induced by the 1000 or 100 sonications repeated at 1 kHz respectively used in [1] and [8].

Fig. 1 clearly shows that the necessary replacement of the agent causes global differences between trials. The arrows indicate where scatter responses occurring early in the channel are destructively interfering with, and changing the shape of, the strong front wall reflections from the initial channel boundary. The *BROAD CHANNEL* (bounded by *red lines*) covers all agent responses undistorted by wall reflections. The phantom channel is wide enough to allow the appearance of multiple scatter responses both longer and shorter than the single applied 400 ns sonication whose length matches that of the *NARROWCHANNEL* (bounded by *black lines*).

We have observed a change in agent longevity when multiple sonications are applied. In this paper we evaluate whether this change is real or an algorithmic artefact that

could introduce inaccuracies when comparing imaging schemes. Such an artefact could arise following minor position shifts between the multiple responses modifying how the real and imaginary components of their individual complex spectra constructively or destructively interfere when forming their combined spectrum generated from the *NARROWCHANNEL* and *BROADCHANNEL* time signals.

II. METHOD

A. Data

The nanobubble study details were captured for sonications of length 10 cycles (400 ns) with a 25 MHz carrier frequency shaped by a Tukey envelope with a flat central response and a roll off to zero intensity over the first and last 10% of the envelope. There was a 1.5 mm diameter agent channel placed in an 11.5 mm wide agar block with sonications excited and responses captured by a confocal transmitter / hydrophone. Trial 1 was performed as part of one study where pressures were increased up to 1000 kPa. Trial 2 was performed as pressures decreased down to 100 kPa with Trial 3 performed during a random pressure selection between 100 and 1000 kPa. Nanobubble agent preparation details are available in [8].

B. Proposed metrics

Following [1] and [8], we determined the area-under-the-curve power spectral metric, AUC_{POWER} , of the phantom channel time signatures

$$AUC_{POWER} = \sum_{f=F_{LOWER}}^{f=F_{UPPER}} A^2(f) \Delta F \quad (1)$$

This was evaluated from the frequency power response, $A^2(f)$, of the excited agent integrated in a bandwidth around

the first harmonic. The frequency resolution, $\Delta F = M / N$, is determined by the A/D sampling rate, M , and the number of points, N , transformed using the discrete Fourier transform, DFT. We followed [8] in windowing and then zero padding the time data before transforming into the frequency domain. These steps respectively reduce the impact of edge distortions, which reduces the spectral amplitude ringing artefacts upon applying the DFT [9], and increase the display resolution via Fourier interpolation [10] to improve the accuracy of determining AUC_{POWER} .

Two metrics were applied. The first calculated the power spectrum generated by transforming the data from the *BROADCHANNEL*, 1.316 ms corresponding to 658 data points. In [8] the agent response signatures were evaluated from a centrally placed time-period, identical in length to the sonication pulse shown schematically as the 400 ns *NARROWCHANNEL* (200 sample points). Given the uneven scatter positions, we replaced this approach by moving an equivalent length data analysis window across the channel in 40 ns steps. This allows the potential capture of both individual and sections of multiple responses as components of the hydrophone signal's short-term Fourier transform (STFT).

III. RESULTS

A. Spectral responses

Figs. 2A, 2B and **2C** respectively show the changes occurring in the spectral response from the nanobubble contrast agent for 30 excitations of every 3rd sonication from Trials 1, 2 and 3 at 500 kPa. Trial 1's spectrum shows a single peak just below the 25 MHz excitation frequency. Trials 2 and 3

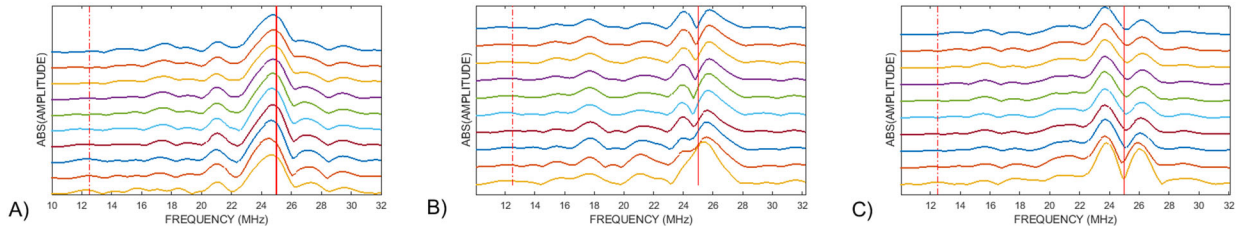


Fig. 2) At 500 kPa, *BROADCHANNEL* agent responses on A) Trial 1 shows a major spectral peak slightly below the sonication carrier frequency of 25 MHz (*solid red line*). In contrast B) Trial 2 responses start with an initial major spectral peak just above 25 MHz which, as sonications continue, changes significantly into a double peak with no spectral component at 25 MHz. C) Trial 3 never shows a significant spectral component at the 25 MHz sonication carrier frequency. The peak offsets and splitting are occurring as the real and imaginary components of the spectra from the multiple responses in the phantom channel constructively or destructively interfere to change the spectral shape.

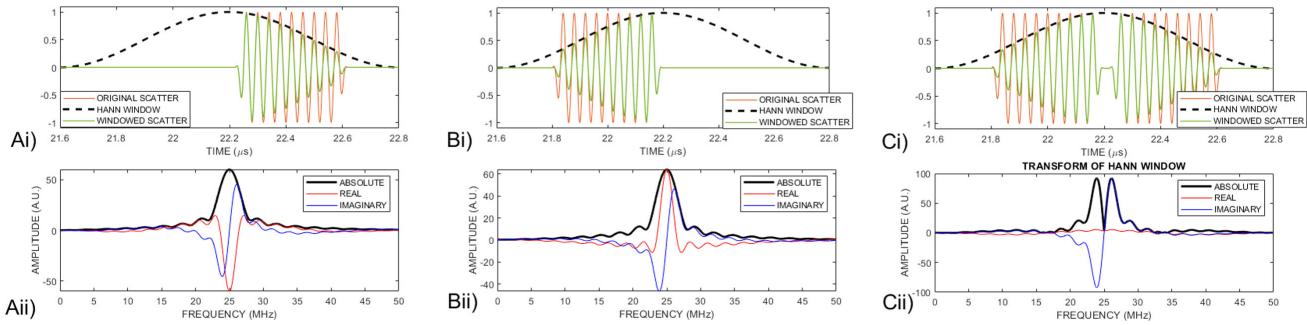


Fig. 3. Two scatter responses Ai) and Bi) (green line), positioned at different locations in the channel have similar absolute (black line) and imaginary (blue line) components of their complex-valued spectra, Aii) and Bii). However, their opposite signed real components (red line) destructively interfere in the combined spectrum Cii) to near zero when both responses are in the channel Ci). This leaves behind a multiple peaked spectrum, the absolute value of the constructively interfering imaginary spectral components.

show spectra with twin peaks split by 3 MHz on either side of the sonication frequency.

Fig. 3 schematically shows why the spectra in **Fig. 2** may not have a spectral peak at the 25 MHz carrier frequency of the single applied sonication. Consider two scatter responses positioned at different locations in the channel (**Figs. 3Ai** and **3Bi**). Their respective complex spectra have near identical absolute (black) and imaginary (blue) components but opposite signed real (red) components, **Figs. 3Aii** and **3Bii**. When both responses are present in the channel (**Fig. 3Ci**) their real spectral components destructively interfere to a near zero value (**Fig. 3Cii**). The absolute value of their constructively interfering imaginary components leaves a double peak either side of the 25 MHz sonication frequency. The changes in the relative intensities of the double peaks in **Figs. 2B** and **2C** are associated with minor alterations in the relative positions of the multiple responses within the channel which modifies their levels of constructive or destructive interference.

Fig. 4 shows how the spectral shape changed when the **NARROWCHANNEL** STFT analysis window was moved across the phantom channel for the 5th Trial 3 sonication. The single peak (light blue line) occurred when the STFT window initially fully enclosed one part of the scatter response. The double peaks indicate where the analysis window captured parts of two responses. Initially the stronger peak is above 25 MHz (magenta dashed-dotted line) later the stronger peak is below 25 MHz (light blue dash-dotted line). Double peaks coalescing into a single offset peak produced the strong dark blue peak near 23 MHz like that seen in **Fig. 2A**, a shift of approximately 10% from the carrier frequency.

There are intensity changes in the spectra at 12.5 MHz (dashed red line). It is difficult to determine whether these should be interpreted as (i) a subharmonic component present whenever a strong first harmonic is present, (ii) the DFT distortion known as spectral leakage [9] associated with the

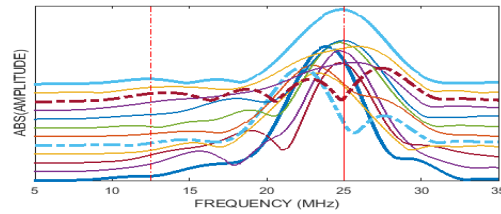


Fig. 4. As the position of the **NARROWCHANNEL** STFT analysis window moves across sonication 5 in Trial 3, the spectral peak is initially centered at the 25 MHz carrier frequency light blue lines, splits into two major peaks, dot-dashed lines, before becoming a single strong 23 MHz peak, dark blue line, offset by approximately 10% from the sonication excitation frequency.

broad-band side-lobes of the transform of the Tukey envelope of the sonication whose strength will change in proportion to the intensity of the strong single peak or less intense dual peaks near 25 MHz or (iii) a combination of both interpretations.

B. Comparison of metrics with multiple responses present

Fig. 5A compares the changes in agent longevity across the three trials following 30 sonications repeated every millisecond measured using the **AUC_{POWER}** spectral power metric determined across the **BROADCHANNEL** region. Despite their different spectral shapes in **Fig. 2**, Trials 2 (magenta) and 3 (gold) show similar responses – a rapid change in agent response with a time constant of around 2.5 milliseconds towards a steady state longevity. In contrast, Trail 1 shows no significant change to multiple sonications, which matches the unchanging spectral characteristics seen in **Fig. 2A**.

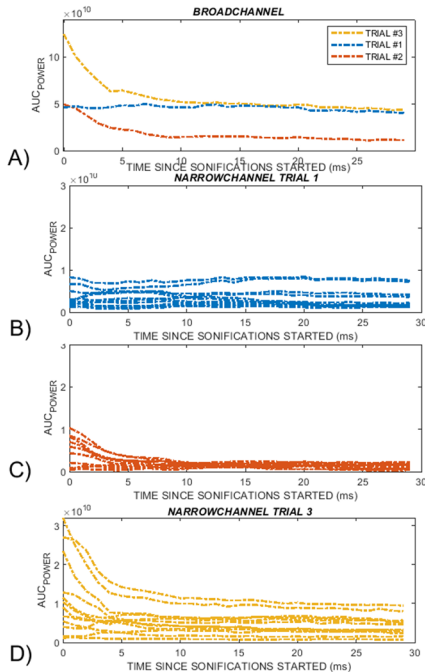


Fig. 5. A) The *BROADCHANNEL* results for Trial 2 (*magenta*) and Trial 3 (*gold*) show a significant change in agent longevity to multiple sonications over 30 milliseconds, but not in Trial 1 (*blue*). B) Trial 1 shows no changes but C) Trial 2 and D) Trial 3 show either an initial or no longevity change depending on the position of the *NARROWCHANNEL* STFT window position within the channel.

Figs. 5B, 5C and 5D respectively show AUC_{POWER} metrics for Trials 1, 2 and 3 as the *NARROWCHANNEL* analysis window was moved across the phantom channel from the end of the front wall reflection to the start of the rear wall reflection. The *NARROWCHANNEL* results for Trial 1 show a similar no change result to the Trial 1 *BROADCHANNEL* metric. For some positions of the moving *NARROWCHANNEL* STFT window of Trials 2 and 3, there is a similar change to the agent's *BROADCHANNEL* responses to sequential sonications. However, the flat responses seen with many of the other STFT window positions responses suggests that the complete set of results reflect a combination of true changes in the longevity plus an additional effect that changes with the relative position of multiple scatter components which produces a spectrum with split peaks rather than a single peak at the excitation frequency.

IV. CONCLUSIONS

Multiple scatter responses were frequently observed in a phantom channel containing a nanobubble contrast agent following a single sonication. We demonstrate how the real and

imaginary components of the complex-valued frequency spectra of individual scatter responses can sum together in a constructive or destructive manner. This can cause the expected single peak at the sonication's carrier frequency to split into multiple peaks depending on the relative positions of the responses in the phantom channel. We compared two spectral power measures; one using all undistorted data in the phantom channel, the other generating spectra from a STFT window the length of the sonication pulse moved across the phantom data. Both measures show that the nanobubble agent longevity can drop with a 2.5 millisecond time constant to a steady state following multiple sonications. However, many positions of the STFT show no longevity changes. We conclude that the spectral power metric can be impacted by both changes in the actual agent response and changes in the relative positions of the multiple scatter responses during a study which can change the shape of the spectrum from a single peak at the sonication frequency to lower intensity multiple peaks.

CONFLICT OF INTEREST

The authors declare that they have no conflict of interest.

REFERENCES

1. R. Eckersley, C. T. Chin and P. N. Burns, "Optimising phase and amplitude modulation schemes for imaging microbubble contrast agents at low acoustic power," *Ultrasound Med Biol*, vol. 31, no. 2, pp. 213-219, 2005.
2. J. Hwang and D. Hope Simpson, "Two pulse technique for ultrasonic imaging". U.S.A. Patent 5951478, 1999.
3. D. Hope Simpson, C. T. Chin and P. N. Burns, "Pulse inversion Doppler: A new method for detecting nonlinear echos from microbubble contrast agents," *IEEE Trans Ultrason Ferroelectr Freq Control*, vol. 46, pp. 372 - 382, 1999.
4. G. Brock-Fisher, M. Poland and P. Rafter, "Means of increasing sensitivity in non-linear ultrasound imaging systems". U.S.A. Patent 5577505, 1996.
5. V. Mor-Avi, E. G. Caiani, K. A. Collines, C. Korcarz, J. Bednarz and R. M. Lang, "Combined Assessment of myocardial perfusions and regional left ventricular function by analysis of contrast enhanced power modulation images," *Circulation*, vol. 104, no. 3, pp. 352 - 357, 2001.
6. B. Haider and R. Y. Chiao, "High order nonlinear ultrasonic imaging," *J Acoust Soc Am Ultrason Symp*, pp. 1527 - 1531, 1999.
7. P. Philips, "Contrast pulse sequences (CPS): Imaging nonlinear microbubbles," *IEEE 2001 Ultrason Symp*, p. 1739-1745, 2001.
8. C. Pellow, J. Tan, E. Cherin, E. Demore, G. Zheng and D. E. Goertz, "High frequency ultrasound nonlinear scattering from porphyrin nanobubbles," *Ultrason*, vol. 110, p. 10625, 2021.
9. F. J. Harris, "On the Use of Windows for Harmonic Analysis with the Discrete Fourier Transform," *Proc IEEE*, vol. 66, pp. 51-83, 1978.
10. M. R. Smith, S. Khan and L. Curiel, "Investigation of hardware and software techniques to enhance the characteristics of focused ultrasound (FUS) spectra," *Phys Med Bio*, vol. 67, pp 145015, 2022